International Journal of Mining Science and Technology 30 (2020) 25–31

Contents lists available at ScienceDirect

International Journal of Mining Science and Technology

journal homepage: www.elsevier.com/locate/ijmst

A case study of the stability of a non-typical bleeder entry system at a U.S. longwall mine

T.M. Klemetti [a,*], M.A. Van Dyke [a], I.B. Tulu [b], D. Tuncay [b]

[a] NIOSH Pittsburgh Mining Research Division, Pittsburgh 15236, USA
[b] Department of Mining Engineering, West Virginia University, Morgantown 26505, USA

ARTICLE INFO

Article history:
Received 9 April 2019
Received in revised form 8 August 2019
Accepted 16 October 2019
Available online 28 January 2020

Keywords:
Abutment loading
Longwall
Instrumentation
Bore hole pressure cells
Pillar loading
Yield pillar
Bleeder pillar

ABSTRACT

Longwall abutment loads are influenced by several factors, including depth of cover, pillar sizes, panel dimensions, geological setting, mining height, proximity to gob, intersection type, and size of the gob. How does proximity to the gob affect pillar loading and entry condition? Does the gob influence depend on whether the abutment load is a forward, side, or rear loading? Do non-typical bleeder entry systems follow the traditional front and side abutment loading and extent concepts? If not, will an improved understanding of the combined abutment extent warrant a change in pillar design or standing support in bleeder entries? This paper details observations made in the non-typical bleeder entries of a moderate depth longwall panel—specifically, data collected from borehole pressure cells and roof extensometers, observations of the conditions of the entries, and numerical modeling of the bleeder entries during longwall extraction. The primary focus was on the extent and magnitude of the abutment loading experienced due to the extraction of the longwall panels. Due to the layout of the longwall panels and bleeder entries, the borehole pressure cells (BPCs) and roof extensometers did not show much change due to the advancing of the first longwall. However, they did show a noticeable increase due to the second longwall advancement, with a maximum of about 4 MPa of pressure increase and 5 mm of roof deformation. The observations of the conditions showed little to no change from before the first longwall panel extraction began to when the second longwall panel had been advanced more than 915 m. Localized pillar spalling was observed on the corners of the pillars closest to the longwall gob as well as an increase in water in the entries. In addition to the observations and instrumentation, numerical modeling was performed to validate modeling procedures against the monitoring results and evaluate the bleeder design. ITASCA Consulting Group's FLAC3D numerical modeling software was used to evaluate the bleeder entries. The results of the models indicated only a minor increase in load during the extraction of the longwall panels. These models showed a much greater increase in stress due to the development of the gateroad and bleeder entries--about 80% development and 20% longwall extraction. The FLAC3D model showed very good correlation between modeled and expected gateroad loading during panel extraction. The front and side abutment extent modeled was very similar to observations from this and previous panels.

1. Introduction

There are two primary underground coal mining methods currently being employed in the United States--the room-and-pillar method and the longwall method. The room-and-pillar method can be broken into two categories: development and retreat. Longwall mining can also be broken into two categories, retreat and advance, where the coal mines in the United States only utilize the retreat method. In the retreating longwall mining method, there are entries developed across the width of the panel at the back end of the panel to support ventilation. These are referred to as bleeder entries. In the design of longwall panels and surrounding pillars and entries, a typical desire is to make the majority of the pillars and openings uniform. When variable pillar dimensions or entry sizes and shapes, relative to those nearby, are found, often stability issues arise. Several bleeder entry systems have been studied previously by researchers [1,2]. These bleeder systems had relatively symmetrical pillars and entry designs that led to even stress redistribution. A non-typical bleeder

* Corresponding author.
E-mail address: tjk6@cdc.gov (T.M. Klemetti).

https://doi.org/10.1016/j.ijmst.2019.12.002
2095-2686/

layout typically occurs due to panel orientation needs relative to property boundaries, past mining, and sometimes surface structures.

This study of a non-typical bleeder entry system was intended to evaluate the effectiveness of the current layout, determine the optimal design for future bleeder designs, and evaluate the load transfer at this site compared to the 21-degree abutment angle concept. The study was focused on the roof and pillar conditions for the given pillar and support designs. This particular site would be exposed to a rear abutment and a partial side abutment from the first and second panel, respectively. The study includes geological assessment, condition monitoring, instrumentation, and numerical modeling. The study began on 9/20/2017 when the initial geological assessment, condition mapping, and instrumentation installation began shortly thereafter. This study was conducted by researchers from the National Institute for Occupational Safety and Health (NIOSH).

1.1. Overall mine and geologic setting

The mine observed in this study utilizes the longwall mining method. Fig. 1 shows the general mine layout with the yield-abutment-yield gateroad design. The longwall panels are retreated from bottom to top and left to right in Fig. 1. The yield pillars are 13 m by 49 m center to center, and the abutment pillars are 50 m by 91 m center to center with 6 m entry widths. The longwall panels are 305 m by 2134 m. The mining height averages 2.4 m with a maximum of 4.5 m. The depth of cover ranges from 335 to 670 m with the cover at the study site panels ranging from 365 to 460 m. The primary support installed was 1.8 m fully grouted number 6 bar on 1.2 m spacing, and there were 2.4 install l2 bolts in the intersections. The study area was not required to utilize any standing support, although some standing supports were installed as instrumentation.

The mine operates within the Blue Creek and Mary Lee coal seams. Both coal seams are within the Black Warrior COAL BASIN in the Pennsylvanian system of the Upper Pottsville group within the New River Formation. The geology within the Mary Lee Coal Group (Fig. 2) contains cyclic layers of coal sandstone and shale intervals. Thick sandstone intervals and silty to sandy shales suggest an upper delta environment. The upheaval of the rocks in the mine have created systematic normal faults that contain 1.5 to 58 m of vertical throw and approximately run in a N28°W direction [3]. The mine tends to plan the mine openings around the major fault systems. The Blue Creek and Mary Lee seams can be separated by as much as 7.62 m and can cause roof control problems when the Mary Lee comes within the bolting horizon. In various areas of the mine property, the Mary Lee Seam is within 0.3 to 1 m of the Blue Creek seam, which allows both seams to be mined simultaneously.

As noted in Fig. 2, coal thickness is exaggerated.

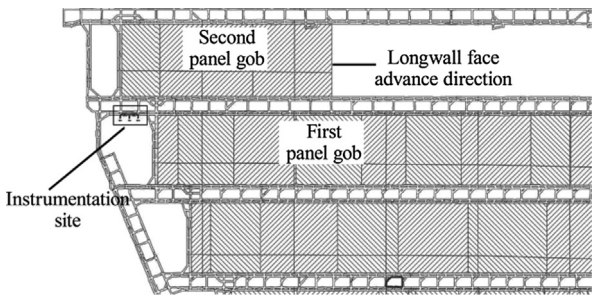

Fig. 1. Global mine layout showing three panels with the gate-road and bleeder layouts.

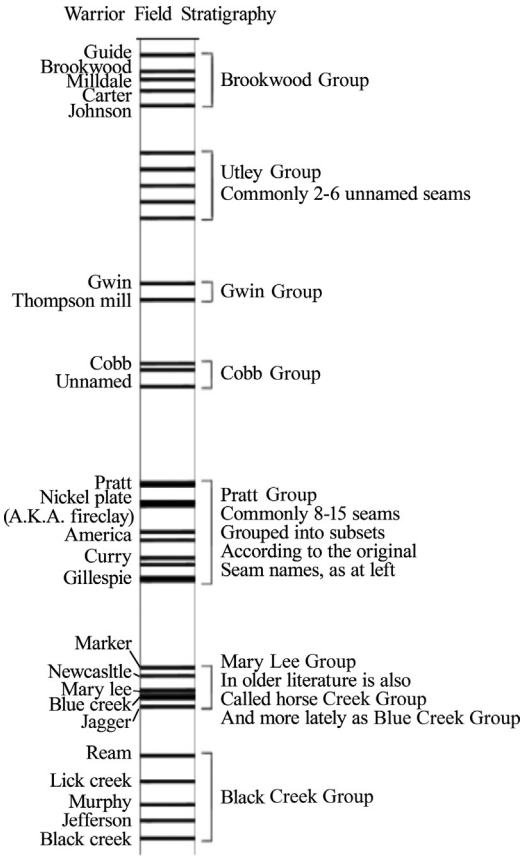

Fig. 2. General stratigraphic column of the Warrior Field, including the Mary Lee Group, representative of the typical mine-wide geological setting.

2. Field study site

2.1. Local geologic setting

A 6.1 m fiberscope was utilized to observe the local roof geology of the instrumented site (Fig. 3). The geology consisted of alternating layers of silty shale and sandstones. The top of the observation hole consisted of a thinly bedded silty shale that was on average 0.43 m thick. Below the silty shale, a 4.9 m thick sandstone body was observed. The sandstone is noted to be thinly bedded to laminated with shale and coal streaks in the upper and lower extents, while the middle 3.8 m of the sand body is medium bedded and relatively stronger. The bottom 0.76 m is silty shale to the roofline.

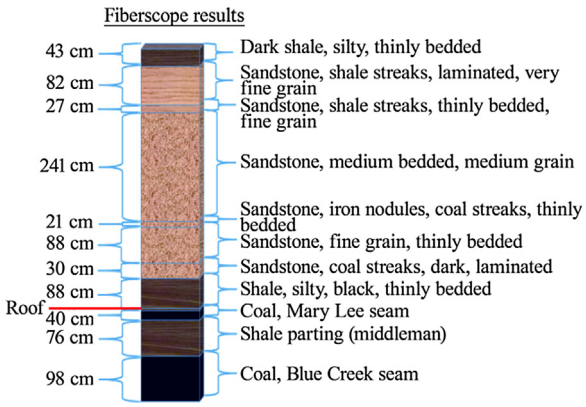

Fig. 3. Fiberscope results of a scope hole within the instrumentation site showing mostly sandstone roof.

The rib geology consists of an average of 7.6 to 12.7 cm of silty shale from the roofline. Below the shale is the Mary Lee Coal Seam that measured 38.1 cm thick and a binder below the coal, known locally as the middle man that was 76.2 cm thick. Under the middle man is the main minable bench of the Blue Creek Coal Seam, which averaged 119 cm at the instrumented site.

2.2. Instrumentation layout

The instrumentation consisted of three roof extensometers (RFEXTs) and three borehole pressure cells (BPCs) as seen in Fig. 4. The BPCs were installed into the rib of the barrier pillar at mid-height of the pillar at a depth of 12.2 m. The location of each BPC was directly across from subsequent crosscuts. The RFEXTs employed four anchors at heights of 0.9, 2.7, 4, and 6.1 m centered in the entry adjacent to the BPC. The RFEXTs and BPCs were recorded using MIDAS dataloggers. Between the roof extensometers and the BPC sites, there were 6.1 m scope holes for immediate roof geologic assessments. In addition, condition mapping of the instrumentation area and surrounding area was conducted, focusing on the #1 entry (area enclosed in black outline in Fig. 4). The instrumentation installation and initial condition mapping were performed within a month of development and less than two weeks prior to the first longwall panel beginning retreating. The intended monitoring period for this study site began upon instrumentation installation and continued through the mining of the next two longwall panels. The period focused on the first panel startup, the middle of the first panel, second panel startup, the middle of the second panel, third panel startup, and the middle of the third panel.

As noted in Fig. 4, clockwise from top left is as Exto-15, Exto-16, and Exto-17.

2.3. Field study results

There are three primary results to discuss, including the roof extensometers, the borehole pressure cells, and the condition mapping. The three roof extensometers (15, 16, and 17 as shown in Fig. 4 from left to right) showed very little movement since their installation, as seen in Fig. 5. RFEXT 15 measured almost no movement during the monitoring period, RFEXT 16 measured an increase of 0.23 cm during the first 915 m of retreat of the first panel, and RFEXT 17 measured a maximum increase of 0.5 cm during the first 915 m of retreat of the second panel. The maximum total movement to date is 0.68 cm with the majority of the roof sag occurring during the first 915 m of retreat of the second panel.

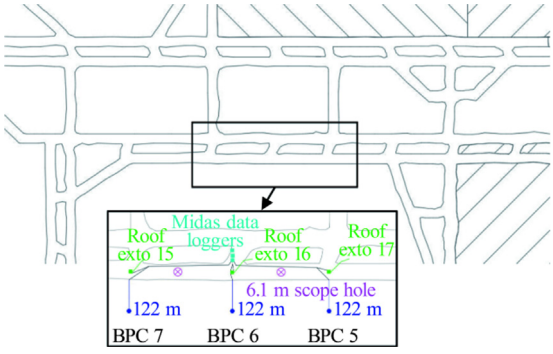

Fig. 4. Instrumentation layout, first panel bleeder site.

The BPCs each responded slightly differently as seen in Fig. 6. BPC 6 and BPC 7 appeared to increase slightly about two weeks after they were initially installed and immediately following second panel startup. The first panel increase of BPC 6 and 7 were 1 and 1.5 MPa, respectively, and the second panel increases of BPC 6 and 7 were 2 and 4 MPa, respectively. The wiring of BPC 5 appears to have been damaged just as the second panel started retreating and is no longer providing meaningful data. BPC 6 appeared to be reading well and matches the observed pressure gauge underground. The electronically recorded reading of BPC 7 was higher than the reading of the pressure gauge mounted inline with the pressure transducer and is very sporadic, most likely due to wiring as well. The BPC pressure gauges were manually read by researchers during their the last few trips to the mine site and appeared to be steady at 6.9, 9.6, and 12.9 MPa for BPC 5, 6, and 7, respectively.

The condition mapping has been completed a few times since installation of the instrumentation. The most recent observations, made on 11-8-2018, are very similar to the initial condition mapping. The only differences are localized increases in the observed pillar spalling closest to the gob of the first panel and the amount of water in the entry. The roof conditions are the same as they were during the initial site evaluation and instrumentation installation.

3. Numerical modeling

Numerical modeling is quickly becoming more and more prevalent in mine planning, design, and case analyses. The inherent enhancement in numerical modeling software, computer hardware, and physical phenomenon associated with underground coal mining has highlighted the benefits to inclusion in the advancement of the science of rock mechanics associated with underground coal mining. To further these advancements, numerical models representing this case study were developed using the procedures discussed later in this paper. These models were used to enhance the understanding of the response of the studied gateroad to the extraction of the two adjacent longwall panels. In addition, the calibrated numerical model will be used as the basis of future research endeavors in conjunction with other field data and calibrated models.

3.1. Numerical modeling methods

In this study, a recently developed numerical-model-based approach is used for estimating the changes in both the horizontal

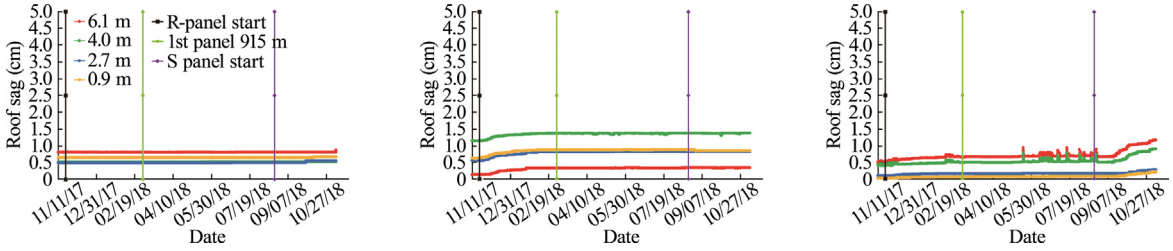

Fig. 5. Roof extensometer data from first panel start to past 915 m of the second panel mined.

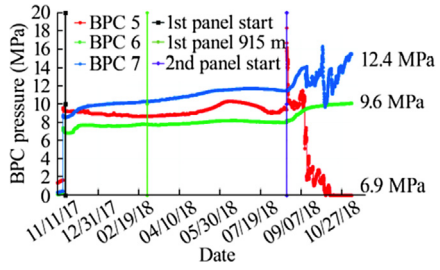

Fig. 6. BPC pressure readings from first panel start through 915 m of second panel retreat.

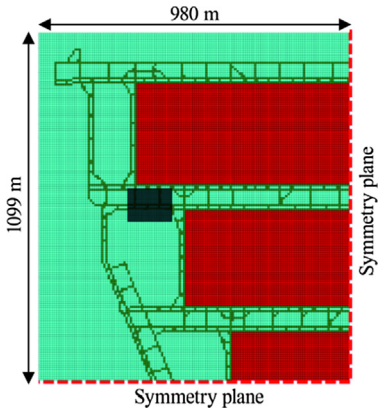

Fig. 7. Plan view of the modeled area showing the increased zone density area of interest.

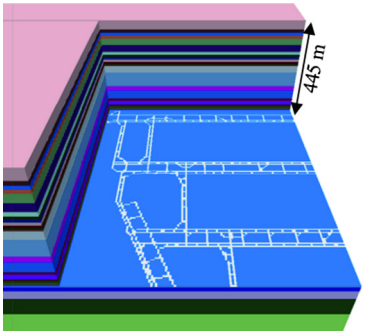

Fig. 8. Image of the modeled geometry and overburden geological sequence.

and vertical loading conditions induced by an approaching longwall face [4]. In this approach, a systematic procedure is used to estimate the model inputs.

Coal is modeled with a Hoek-Brown coal model calibrated by researchers at the NIOSH Pittsburgh Mining Research Division (PMRD) to represent the Mark-Bieniawski equation [5]. The response of the gob is calibrated with back analysis of subsidence data and the results of previously published laboratory tests on rock fragments. The modeling procedures were verified with the subsidence and stress data recently collected by PMRD from a longwall mine in the eastern United States and with published case studies from both eastern and western U.S. mines [4]. These procedures were followed to create a model of the study site using local rock mass parameters and loading conditions.

The overburden in the study area consists of alternating layers of sandy shale, sandstone, fireclay, and coal. Interfaces between the geological layers in the overburden were modeled with interface elements. Coulomb's criterion was used to define the limiting shear strength of the interfaces. As described by Su, the coefficient of friction of interfaces was set to 0.25 [6,7].

In developing the FLAC3D panel scale model, first a 2D model was developed employing actual stratigraphy, using all the geological layers from a nearby core hole with a minimum modeled layer thickness of 1.0 m. This model of the mine had 61 different layers with thicknesses ranging from 1.0 to 26.0 m to simulate the overburden. The 2D model results were compared with the Virginia Polytechnic Institute and State University (VPI) empirical subsidence prediction program, the Surface Deformation Prediction System (SDPS) [8,9]. The FLAC model approximated subsidence of the panel with average overburden depth of 441 m, panel width of 305 m, and a hard-rock ratio of 32% as 1.39 m compared to the SDPS prediction of 1.26 m. The 2D model had approximately 1.0 million elements. In order to generate a 3D model that can run in a reasonable time frame, the minimum thickness of elements on the overburden increased to 7.0 m. In order to generate a 3D model that can approximate stresses accurately with larger elements, overburden lithological layers with the same rock type with thickness less than 7.0 m were combined and represented with a transversely isotropic material model. The 3D model of the mine had 30 different layers and approximately 1.16 million elements. The 3D model's initial grid was developed by taking the grid generated from the stability mapping grid generator developed for the LaModel software program and then converting it to FLAC3D grid with a custom visual basic program [10] . The instrumented pillars, roof, and floor were simulated with 1.0 m elements in the detailed area as shown in Fig. 7. Fig. 7 shows two stages of increasing zone density, the first at the black rectangle in Fig. 7 encapsulating the entire study area. The second stage is near the mid-pillar site, centered on the yield pillar and part of the adjacent abutment pillar. The geometry of the model with the representative geological sequence that was modeled is shown in Fig. 8.

3.2. Numerical modeling results

The numerical model was solved for three stages, the first being development, the second being the complete retreating of the first panel, and the third being the complete retreating of the second panel. The primary modeling results of interest to this study are that of the stress redistribution and rib yielding depth due to longwall extraction. The global stress redistribution due to the three evaluation stages of the numerical model can be seen in Fig. 9 as a global view of the vertical stress results for the three stages modeled. The entries mined for the development stage produce an increase in the stresses near the entries. The majority of the stress changes for the first and second panel retreating are localized to the gateroads and other nearby solid coal elements. To better see the changes in the stresses in the study area, a local stress plot is shown in Fig. 10. Fig. 10 shows stress concentrations in the corner of the gateroad and barrier pillars closest to the gob. The instrumented area and the yield pillars only show minor increases compared to the abutment pillars nearest the developed gob.

Another interesting result of the modeling effort is that of the gateroad/bleeder entry pillar stress changes due to the first and second panel retreat. Fig. 11 shows the entire model, a zoomed-in view of the study area, and a table of the average pillar stresses for the three stages modeled. The study area included four yield pillars and one abutment pillar. The yield pillars showed relatively minor stress increase due to both the first and second panel retreat. The first panel retreating resulted in an average increase of 1.2 MPa for the yield pillars in the study area. The second panel actually caused the loading of the yield pillars to exceed their peak strength, resulting in a decrease in the average pillar stress of 0.5 MPa as they started to yield. The abutment pillar exhibited

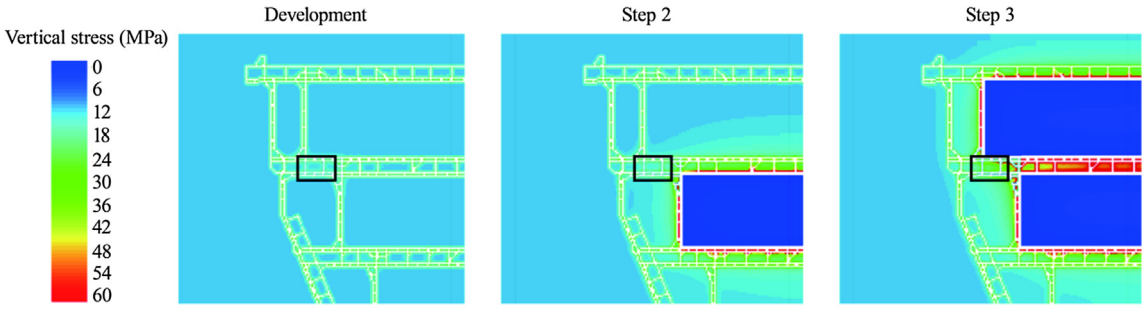

Fig. 9. Global view of the vertical stress results for the three stages modeled.

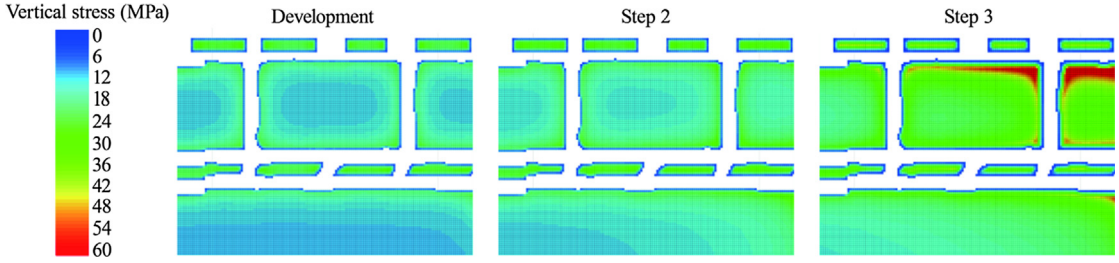

Fig. 10. Local view of the vertical stress results for the three stages modeled.

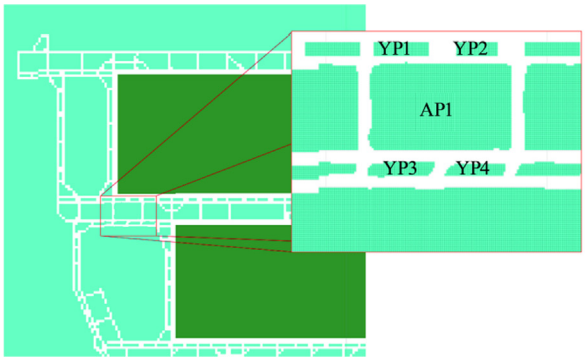

	Average pillar stress (MPa)				
	AP1	YP1	YP2	YP3	YP4
Dev.	-14.34	-17.19	-17.06	-17.51	-15.89
Step 1	-16.06	-18.21	-18.29	-18.99	-16.77
Step 2	-27.39	-17.30	-16.49	-20.23	-15.52

Fig. 11. Location of the yield pillars in the study area and the change in stresses due to mining.

an average increase in stress of 1.7 and 11.3 MPa due to the retreating of the first and second panel, respectively.

The rib yielding depth was determined by evaluating the yield of the modeled coal elements in each model stage for the zones in the yield pillars of the study area. The rib yielding for all four yield pillars and the abutment pillar in the study area showed yielding to a depth of 2 m upon development as shown in Fig. 12. The retreating of the first panel resulted in an increase of yielding to a depth of 3 m for the yield pillar closest to the newly formed gob. The retreating of the second panel resulted in complete yielding of the other three yield pillars and an increase of yielding to 3 m for the yield pillar closest to the first gob. The abutment pillar showed no increase in yielding due to the first panel retreating; however, it did experience an increase in yielding to 3.5 m due to the second panel retreating.

4. Discussion

4.1. Modeling and instrumentation comparison

To date, the roof extensometers indicate that the roof is competent and strong enough to withstand the stresses imposed in this layout. The roof sag appears to be related to the first several hundred or thousand meters of advancement of each subsequent panel. The maximum roof sag measured at this site is just slightly greater than 6.8 mm, much less than the established 25.4 mm trigger for additional support [11]. The general Australian Tarp requirement is on the order of 50 mm. For the majority of the area being evaluated, the roof has seen little time-dependent movement or deterioration, a positive sign for long-term stability of the entry.

Two of the BPCs have shown an increase in pressure associated with the startup or squaring of the first and second panel. One BPC showed a 4 MPa increase during the first 915 m of the second panel retreating. The other showed the majority of the increase during startup of the first panel, although it did increase in pressure steadily during the mining of the first panel. The third BPC actually showed a massive decrease, most likely due to a wiring issue; however, the pressure gauge attached to the BPC shows that the pressure has remained constant during the entire monitoring period. These readings are indicative of a relatively stable pillar accommodating the stress increase caused by the extraction of coal in the longwall panel in relatively close proximity to the pillars being monitored.

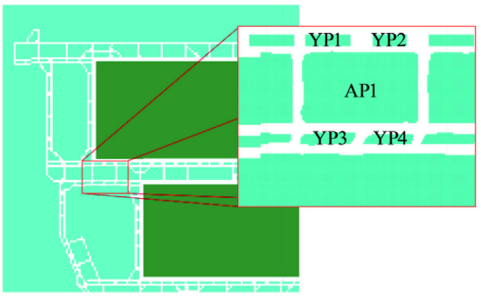

	Yield depth (m)				
Dev.	2	2	2	2	2
Step 1	2	2	2	2	3
Step 2	3.5	-	-	3	-

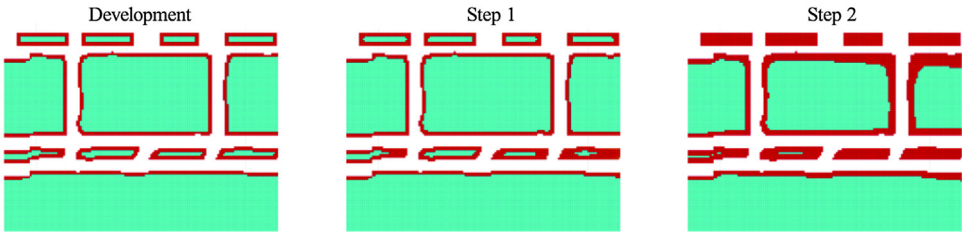

Fig. 12. Modeled area, yielding of the study area, and resulting average depth of yielding in the study area.

The combined BPC loading, roof extensometer measurements, and condition mapping indicate a very stable design, especially considering the lack of standing support in this area. Similar evaluations have been performed at other mines, providing results that indicate very stable designs are implemented in which standing supports are only exposed to about 30%-40% of their load capacity.

The modeling replicated the instrumentation and monitoring results fairly well. There was little to no displacement in the modeled roof; the modeled stress increases were similar for the first panel and slightly greater for the second panel. The model provided reasonable results in terms of pillar rib yielding and yield pillar response to longwall panel retreating. Importantly, the models correctly showed that the overall pillar layout was stable, that the yield pillars yield in a controlled manner, while the entries were also predicted to require minimal support, as observed in the mine. The standardized modeling procedures used in this study are, therefore, likely to be sufficient to assess future longwall and bleeder entry layout options at this mine.

4.2. Difficulties and obstacles of instrumentation at bleeder sites

The attempt to measure the response of the bleeder pillars, entry, and supports to the developed longwall gob showed several areas for improvement and highlighted potential obstacles and difficulties in acquiring the desired data set. There are several practical limitations affecting the ability to collect the desired measurements in this site and similar sites. The first is the amount of time available to install the instruments due to the production needs and mine progression. Bleeder sites like this one are often developed a short time before moving the longwall equipment and beginning the retreat of the longwall panel. In this case, the bleeder entry development was completed less than two weeks prior to the beginning of longwall retreat, and the moving of the shields, panline, shearer, and other longwall mining equipment began immediately upon completing development of the start-up room or during mining of the remaining bleeder entries.

In addition to having to deal with a very short installation window, the first critical monitoring period begins as soon as the longwall begins retreating. This can cause difficulties in verifying the operating status of all monitoring instruments and limit the time to troubleshoot any abnormalities or malfunctioning instruments. With all the production activity occurring in the study area, something as simple as tracing wires to ensure proper wiring sequence can be seem nearly impossible in the one-week window available. If the malfunctioning instrument is determined to be the instrument itself rather than the wiring or datalogger, there may not be equipment available to drill holes to install new instruments, let alone time to order, prepare, or calibrate the new instrument.

The proximity of the study mine to the researcher, consultant, or mine employees' home office can also present difficulties in obtaining quality-complete data sets. Because of the cost and time of traveling farther and farther away from the office, a balance between the need to continually observe the instruments and the cost of resources must be made. Ideally, there would always be someone available to collect data, observe the entry conditions, and troubleshoot as necessary; especially during the critical monitoring periods of the panel startup and nearby mining. For the bleeder entry studies, the critical monitoring period typically lasts 2 months or more, while the face advances 1000 m.

5. Future work

Although this assessment only includes the instrumentation and mine observations through the first panel and the first thousand or so meters of the second panel, there is adequate information to demonstrate the effectiveness of this bleeder design used in the study area. Future monitoring will record the long-term stability of this design and provide an indication of the time-dependent deformation and stress changes. Additional investigation of different bleeder designs under different depths of cover and different geological settings using the validated numerical model will provide the ability to forecast the effectiveness of bleeder designs within the bounds of the varied conditions studied. The results of this and future studies will provide mine workers with optimized bleeder pillar and support designs.

6. Disclaimer

The findings and conclusions in this report are those of the author(s) and do not necessarily represent the official position of the National Institute for Occupational Safety and Health, Centers for Disease Control and Prevention. Mention of any company or product does not constitute endorsement by NIOSH.

References

[1] Klemetti TM, Van Dyke MA, Tulu IB. Deep cover bleeder entry performance and support loading: a case study. Int J Min Sci Technol 2018;28(1):85–93.

[2] Mishra B, Tang X. Stability analyses of bleeder pillars in longwall mines by displacement-discontinuity method. Int J Min Sci Technol 2015;25(6):933–41.
[3] Murrie GW, Diamond WP, Lambert SW. Geology of the Mary Lee Group of Coalbeds, Black Warrior Coal Basin, Alabama. In Report of Investigations 8189. United States Department of the Interior. Bureau of Mines. 1976.
[4] Tulu IB, Esterhuizen GS, Gearhart D, Klemetti TM, Mohamed KM, Su DWH. Analysis of global and local stress changes in a longwall gateroad. Int J Min Sci Technol 2018;28(1):127–35.
[5] Esterhuizen E, Mark C, Murphy M. The ground response curve and its impact on pillar loading in coal mines. In: Proceedings of the 3rd International Workshop on Coal Pillar Mechanics and Design. p. 123–31.
[6] Su DWH. Finite element modeling of subsidence induced by underground coal mining: the influence of material nonlinearity and shearing along existing planes of weakness. In: Peng SS, editor. Proceedings of the 10th International Conference on Ground Control in Mining. Morgantown, WV: West Virginia University; 1991. p. 287–300.
[7] Su DWH. Personal communication; 2016.
[8] Karmis M, Jarosz A, Agioutantis Z. Predicting subsidence with a computer. Coal 1989;26(12):54–61.
[9] Agioutantis Z, Karmis M. Quick Reference Guide and Working Examples, SDPS for Windows, Version 6.2J. 2017.
[10] Wang Q, Heasley K. Stability mapping system. In: Proceedings of the 24th International Conference on Ground Control in Mining. Morgantown, WV: West Virginia University; 2005. p. 243–9.
[11] Barczak TM, Tadolini S, Zhang P. Evaluation of support and ground response as longwall face advances into and widens pre-driven recovery room. In: Peng SS, editor. Proceedings of the 26th International Conference on Ground Control in Mining. Morgantown, WV: West Virginia University; 2007. p. 160–72.